Journal of Electroceramics, 13, 305–309, 2004

Electrical Properties of 6H-$BaTi_{0.95}M_{0.05}O_{3-\delta}$ Ceramics where M = Mn, Fe, Co and Ni

GILLIAN M. KEITH,[1] KUMARAVINOTHAN SARMA,[2] NEIL MCN. ALFORD[2] & DEREK C. SINCLAIR[1]

[1]*Department of Engineering Materials, University of Sheffield, Sheffield, S1 3JD, UK*
[2]*School of EEIE, South Bank University, London, SE1 0AA, UK*

Submitted March 31, 2003; Revised February 27, 2004; Accepted June 24, 2004

Abstract. Hexagonal $BaTiO_3$ materials have been stabilised at room temperature according to the formula $BaTi_{0.95}M_{0.05}$ $O_{3-\delta}$ where M = Mn, Fe, Co and Ni. Dense ceramics (>96% of the theoretical X-ray density) were sintered at 1450°C in flowing O_2 gas from calcined powders prepared by the mixed oxide route at 1300°C. All samples were single-phase and the bulk conductivity, σ_b, measured by Impedance Spectroscopy and Q.f measured by microwave dielectric resonance methods showed a strong dependence on the type of dopant. σ_b at 300°C was 10^{-7}, $10^{-5.5}$, $10^{-5.5}$ and 10^{-4} Scm^{-1} for M = Mn, Fe, Ni and Co, respectively and Q.f at ~ 5 GHz was 7790, 6670, 2442 and 1291 GHz, for M = Mn, Fe, Ni and Co, respectively. The correlation between σ_b and Q.f is attributed to the presence of oxygen vacancies and/or mixed valency of the dopant ions.

Keywords: $BaTiO_3$, perovskites, microwave dielectric resonators, impedance spectroscopy

Introduction

$BaTiO_3$ has various polymorphs, all of which are based on the perovskite structure (ABO_3); however, due to their high permittivity, ferroelectric (tetragonal) $BaTiO_3$-based materials have received the most attention. In this form, the structure consists of pseudo-cubic close packed BaO_3 layers with corner sharing between the TiO_6 units and this type of structure is often referred to as a 3C-type perovskite (Fig. 1(a)). Surprisingly, very little is known about the electrical properties and defect chemistry of the high temperature hexagonal (6H) polymorph which is stable above ~1430°C in 'undoped' $BaTiO_3$ [1]. Stoichiometric 6H-$BaTiO_3$ crystallises in the space group $P6_3/mmc$ [2] and can be described as pseudo-close packed BaO_3 layers, with a $[cch]_2$ sequence where *c* and *h* refer to cubic and hexagonal stacking, respectively. The Titaniums Ti(1) and Ti(2) occupy corner- and face-sharing octahedra, respectively (Fig. 1(b)). Stoichiometric 6H-$BaTiO_3$ undergoes structural phase transitions on cooling at 220 and ~70 K [3] to give polymorphs with $C222_1$ (orthorhombic) and $P2_1$ (monoclinic) space groups, respectively [4].

To date, 6H-$BaTiO_3$ has been stabilised at room temperature by several methods including; rapid quenching of undoped $BaTiO_3$ from >1500°C, partial reduction of Ti(+IV) to Ti(+III) by heating 3C-type $BaTiO_3$ under low pO_2 at >1300°C [5] and by partial substitution of Ti by various cations, eg Mg, Mn, Ru and Pt [6]. Recently we have undertaken a systematic study of the structure-composition-electrical property relationships in a range of 6H-$BaTiO_3$ materials based on various Ti-site dopants, eg Mg, Al, Ga, In, Mn, Fe, Co and Ni. To date, we have shown that Ga-doped 6H-$BaTiO_3$ ceramics have room temperature permittivity, ε'_{25} of ~70–80 and resonate at microwave frequencies with a quality factor, Q.f of ~7000–8000 GHz at ~5 GHz [7]. In addition, we have used impedance spectroscopy under various oxygen partial pressures to establish the high temperature conductivity behaviour of Ga-doped ceramics [8] which show the presence of a *p-n* transition with slopes of $\sim -1/4$ and $+1/4$ in the *n*- and *p*-type regions indicating that the conductivity obeys the extrinsic model proposed by Smyth and co-workers [9, 10] for undoped and acceptor-doped 3C-$BaTiO_3$ type materials. Here we report and discuss the microwave dielectric properties and high temperature

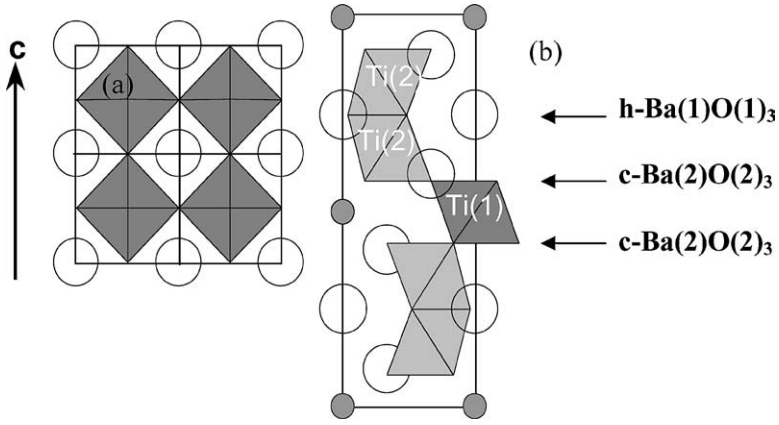

Fig. 1. The 3C (a) and 6H (b) unit cells of $BaTiO_3$. Large open circles represent Ba^{2+} ions, small filled circles represent Ti^{4+} ions. In (b) dark and light shaded octahedra represent $Ti(1)O_6$ and Ti(2)O(6), respectively. For clarity O^{2-} ions are not shown.

conductivity behaviour in air of $BaTi_{0.95}M_{0.05}\ O_{3-\delta}$ ceramics where M = Mn, Fe, Co and Ni.

Experimental

All samples (∼50 g) were prepared by the mixed oxide route from appropriate quantities of $BaCO_3$, TiO_2 and MnO_2, Fe_2O_3, Co_3O_4 or NiO according to the formula $Ba(Ti_{0.95}\ M_{0.05})O_{3-\delta}$ where M = Mn, Fe, Co and Ni. The batches were milled overnight using yttria stabilised zirconia milling media in a polypropylene pot with acetone, calcined overnight at 1300°C and remilled for 16–18 hours. Pellets (8–10 mm in diameter and 2–3 mm thick) were uniaxially cold-pressed in a stainless steel die using a compaction pressure of ∼200 MPa prior to sintering at 1450°C for 2 hours in flowing O_2 at a heating and cooling rate of 5°C/min.

X-ray analysis for phase identification was carried out using a Stoe Stadi P Image Plate (IP) diffractometer with Cu Kα radiation. The phase purity of the powders and of pulverised pellets after sintering was determined using the indexing scheme for undoped 6H-$BaTiO_3$ reported in the ICDD file, card number 34-129. Lattice parameters were calculated using data obtained from a Stoe Stadi P diffractometer using Cu Kα radiation and a position sensitive detector which was calibrated using an external Si standard. The density of sintered pellets was estimated from the mass and dimensions of the pellets compared to that expected from the theoretical X-ray density. Ceramic microstructures were examined by Scanning Electron Microscopy (SEM) using a Camscan Mk2 SEM operating at 20 kV. Microwave dielectric measurements of relative permittivity, $\in$r, and quality factor, Q (=1/tan δ), were performed on ceramic discs by the resonant cavity method using a network analyser, Hewlett-Packard model 8720D and Impedance Spectroscopy was performed on Pt-coated discs in air between ∼25–900°C using a Hewlett-Packard impedance analyser model 4192A operating at 100 mV in the range 5 Hz–13 MHz.

Results

All four compositions were single-phase by X-ray Diffraction and the lattice parameters are given in Table 1. The solid solution limits and crystal chemistry for each dopant series will be reported elsewhere [11]; however, it is important to note that stable Rietveld refinements of powder X-ray and Neutron Diffraction (collected on HRPD at Rutherford Appleton Laboratories) data using the space group $P6_3/mmc$ were obtained for full site occupancy of the O(2)

Table 1. Unit cell parameters for $BaTi_{0.95}M_{0.05}O_{3-\delta}$ and for undoped $BaTiO_3$ [2].

M	a/Å	c/Å
Mn	5.7197 (6)	13.9612 (12)
Fe	5.7236 (7)	13.9918 (17)
Co	5.7200 (6)	13.9869 (13)
Ni	5.7224 (13)	14.000 (3)
Undoped 6H-$BaTiO_3$ [2]	5.7238 (7)	13.9649 (9)

sites; however, occupancies of less than one for the O(1) sites were obtained for Fe-, Co- and Ni-doped samples. No significant level of oxygen deficiency was observed for the Mn-doped sample.

Pellet densities were >96% of the theoretical X-ray density and micrographs of the ceramic microstructures have been published previously [12]. The microstructures of M = Fe-, Co- and Ni-doped ceramics consisted of regular grains with an average grain size between 5–10 μm. For Mn-doped ceramics, the microstructure exhibited exaggerated grain growth with long plate-like grains in excess of 100 μm with low aspect ratios.

Impedance Spectroscopy (IS) data for all four sets of ceramics could be modelled on an equivalent circuit consisting of a single parallel RC element. Typical data in the form of an impedance (Z^*) plane plot are shown in Fig. 2(a) and consist of a single semicircular arc with an associated capacitance (calculated using the relationship $\omega RC = 1$ at $-Z''_{max}$) of $\sim$ 4–6 $pFcm^{-1}$ which is a typical bulk (intra-granular) value based on the brickwork-layer model for electroceramics [13]. Hence, the bulk resistance, R_b, was estimated from the intercept of the arc on the real, Z', axis and the bulk conductivity, $\sigma_b = 1/R_b$. A typical combined Z'' and M'' spectroscopic plot (where $M^* = j\omega C_o Z^*$ and $j = \sqrt{-1}$ and C_o is the vacuum capacitance of the cell) is shown in Fig. 2(b) and consists of a single Debye-like peak with similar values of ω_{max}. As M" spectroscopic plots are dominated by small capacitances this confirms the arc in Z* plots to be associated with the bulk response, confirms the choice of equivalent circuit and demonstrates the ceramics to be electrically homogeneous.

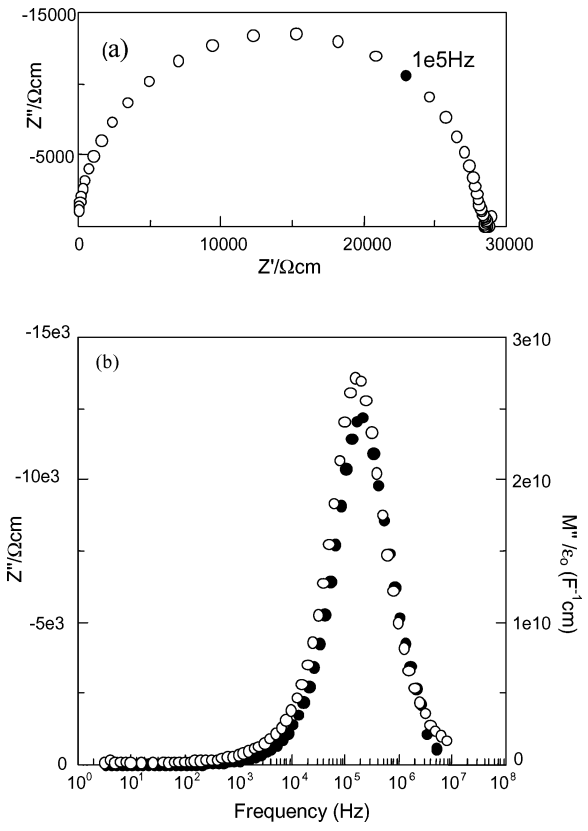

Fig. 2. Z* (a) and combined Z″ (open symbols) and M″ (filled symbols) spectroscopic plot (b) for $BaTi_{0.95}Fe_{0.05}O_{3-\delta}$ at 437°C.

Arrhenius plots of σ_b for samples measured in air are shown in Fig. 3. Although the data show deviations from linear behaviour at lower temperatures, it is clear that the bulk conductivity of Mn-doped ceramics is much lower than that of Ni-, Fe- and Co-doped ceramics, especially at lower temperatures. The activation energy associated with the bulk conductivity was estimated by linear fitting of the higher-temperature data with values of ~1.2, 0.9, 0.9 and 0.5 eV, for Mn-, Ni-, Fe- and Co-doped ceramics, respectively.

ε'_{25} and Q.f values at microwave frequencies are given in Table 2 and show that all ceramics possess high ε'_{25} values (~55–85) that are consistent with that measured at higher temperatures by Impedance Spectroscopy. The Q.f values are rather low (~1300–8000 GHz) but they correlate with the trend observed for the bulk conductivity measured by Impedance Spectroscopy, Fig. 3, i.e. the highest Q.f values are obtained for Mn-doped ceramics whereas the lowest values are obtained for Co-doped ceramics. Although measurements of the temperature coefficient of resonant frequency (TC_f) have yet to be performed, subambient (down to ~80 K) fixed frequency (1 MHz) capacitance measurements show the permittivity to rise substantially at lower temperatures

Table 2. Microwave dielectric properties of $BaTi_{0.95}M_{0.05}O_{3-\delta}$ sintered at 1450°C in flowing O_2 gas.

M	ε'_{25}	f/GHz	Q.f /GHz
Mn	71	4.80	7790
Fe	83	4.73	6670
Co	74	4.30	1291
Ni	56	5.19	2442

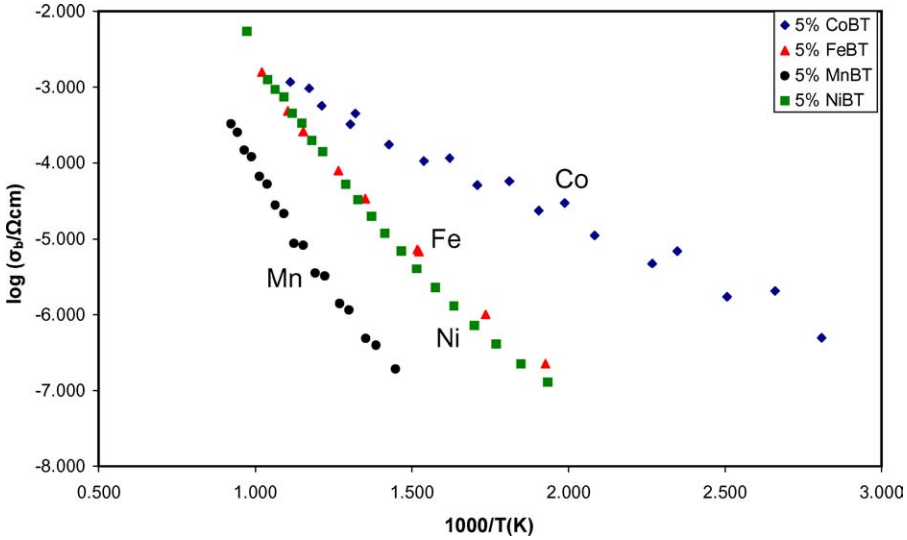

Fig. 3. Arrhenius plots of the bulk conductivity (σ_b) for $BaTi_{0.95}Fe_{0.05}O_{3-\delta}$ where M = Mn, Fe, Co and Ni.

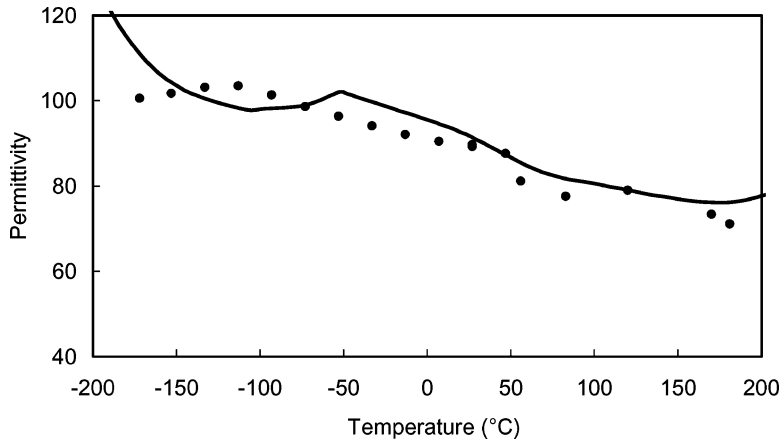

Fig. 4. Permittivity as a function of temperature for undoped 6H-$BaTiO_3$ (line) and $BaTi_{0.95}Fe_{0.05}O_{3-\delta}$ (closed symbols).

suggesting high values of TC_f (>400 $ppmK^{-1}$) are to be expected. For example, Fig. 4 shows that 5% Fe-doping is effective in suppressing the transition at ~220 K in undoped 6H-$BaTiO_3$ ceramics by ~60 K to ~160 K.

Discussion

No noticeable trends in lattice parameters were apparent as a function of the ionic radii of M, Table 1; however, as noted by Grey et al. [14] for M = Fe(+III), the presence of oxygen vacancies on the O(1) sites causes an increase in c and this was apparent for the M = Fe-, Co- and Ni-doped samples in the present study. An in-depth crystallographic report of these samples is beyond the scope of the present paper and will be reported elsewhere [11]; however a notable structural feature is the increase in the Ti(2)-Ti(2) separation within the face sharing Ti_2O_9 dimers of Fe-, Co- and Ni-doped samples compared to undoped and M = Mn 6H-$BaTiO_3$ materials and this can be attributed to the poorer shielding of the M(2) cations from each other as oxygen is removed from the O(1) sites. The contraction of *c* and the lack of any significant oxygen deficiency in the Mn-doped sample is consistent with a size effect where Ti(+IV) is partially replaced by the smaller Mn(+IV) ion.

The bulk conductivity and Q at room temperature are strongly dependent on the type of dopant, Fig. 3 and Table 2, respectively. Mn-doped ceramics have the lowest bulk conductivity with a high activation energy of ∼1.2 eV and the highest Q.f value of all the dopants studied. The activation energy is similar to that reported for undoped 3C$BaTiO_3$ceramics and may be consistent with an extrinsic-type band model. In contrast, Co-doped samples are 'leaky' dielectrics, with a low activation energy of ∼0.5 eV which may be consistent with some polaron hopping mediated conduction mechanism, presumably related to the presence of mixed Co(+II)/Co(+III) in the samples. It should be noted that no low frequency 'spike' indicative of ionic polarisation and diffusion atthe electrodes was observed in the Z* plots at any temperature, thus indicating the conduction (for this level of doping) is predominantly via electronic species as opposed to oxide ion conduction.

Many 'extrinsic' factors are known to influence Q in microwave dielectric measurements, including ceramic microstructure (eg pellet density and average grain-size), secondary phases, etc. [15]. Although we cannot eliminate these 'extrinsic' variables from our ceramics there is a strong and systematic correlation between thepresence of oxygen vacancies and the level of bulk conductivity with the value of Q.f. This suggests that the variation in Q at microwave frequencies in this series of samples, Table 2, is controlled primarily by the bulk composition. Although $\varepsilon'_{25} > 50$ for all the ceramics, the low Q.f values and strong temperature dependence of the permittivity behaviour, Fig. 4, which is presumably related to the presence of the subambientphase transitions reported for un-doped 6H-$BaTiO_3$ preclude any potential commercial applications of these materials as high permittivity dielectric resonators.

Conclusions

A series of $BaTi_{0.95}M_{0.05}$ $O_{3-\delta}$ ceramics where M = Mn, Fe, Co and Ni has been prepared and their electrical properties studied by a combination of Impedance Spectroscopy and microwave dielectric resonance measurements. The results indicate a strong dependence between the bulk conductivity and Q.f with the type of dopant. In particular, M = Mn have the lowest bulk conductivity and highest Q at microwave frequencies and this appears to be related to the absence of any significant level of mixed valence of the Mn ion and/or any significant level of oxygen non-stoichiometry.

Acknowledgments

EPSRC for funding (studentship GMK), Dr C A Kirk (Natural History Museum., London) for useful discussions on Rietveld refinement procedures and Drs Kevin Knight and Ron Smith (both Rutherford Appleton Laboratories) for assistance with thecollection of Neutron Diffraction data.

References

1. K.W. Kirby and B.A. Wechsler, *J. Am. Ceram. Soc.,***74**, 1841 (1991).
2. J. Akimoto, Y. Gotoh, and Y. Oosawa, *Acta. Crystallogr. Sect. C*, **50**, 160 (1994).
3. Y. Akishigue, T. Atake, Y. Saito, and E. Sawaguchi , *J. Phys. Soc. Jpn*., **58,** 930 (1989).
4. Y. Noda, K. Akiyama, T. Shobu, Y. Kuroiwa, and H. Yamaguchi, *Jpn. J. Appl. Phys*., **38**, 73 (1999).
5. D.C. Sinclair, J.M.S. Skakle, F.D. Morrison, R.I. Smith, and T.P. Beales, *J. Mater. Chem*., **9**, 1327(1999).
6. J.G. Dickson, L. Katz, and R. Ward, *J. Am. Chem. Soc*., **83**, 3026 (1961).
7. A. Feteira, K. Sarma, N. Mc. Alford, I.M. Reaney, and D.C. Sinclair, *J. Am. Ceram. Soc.*, **86**, 511 (2003).
8. M.J. Rampling, G.C. Mather, F.M.B. Marques, and D.C. Sinclair, *J. Eur. Ceram. Soc.*, **23**, 1911 (2003).
9. H.M. Chan, R.K. Sharma, and D.M. Smyth, *J. Am. Ceram. Soc*., **64**, 556 (1981).
10. N.H. Chan, R.K. Sharma, and D.M. Smyth, *J. Am. Ceram. Soc*., **65**, 167 (1982).
11. G.M. Keith, PhD Thesis, University of Sheffield (2003).
12. G.M. Keith, M.J. Rampling, K. Sarma, N. Mc. Alford, and D.C Sinclair, *J. Eur. Ceram. Soc.*, in press (2003).
13. J.T.S. Irvine, D.C Sinclair, and A.R West, *Adv. Mater.,* **2**, 132 (1990).
14. I.E. Grey, C. Li, L.M.D. Cranswick, R.S. Roth, and T.A. Vanderah, *J. Solid State Chem.*, **135**, 312 (1998).
15. N. McN. Alford and S.J. Penn, *J. Appl. Phys*., **80**, 5895 (1996).